SCIENTIFIC PAPER

INTEGRATED NEURAL NETWORK AND ASPEN PLUS MODEL FOR ENTRAINED FLOW GASIFICATION KINETICS INVESTIGATION

Dario Balaban[1,2*], Jelena Lubura[1], Predrag Kojić[1],

[1]*University of Novi Sad, Faculty of Technology Novi Sad, Bulevar cara Lazara 1, 21000 Novi Sad, Serbia*

[2]*University of East Sarajevo, Faculty of Technology Zvornik, Karakaj 34A, 75400 Zvornik, Republic of Srpska, Bosnia and Herzegovina*

https://doi.org/10.2298/CICEQ240430032B

Received 30.4.2024.

Revised 27.8.2024.

Accepted 18.9.2024.

*Correspondence:
e-mail: dario.balaban@uns.ac.rs
Telephone number: +381612865507
Fax number: +38121450413

Abstract

Entrained flow gasification is a well-established technology, however, the main obstacle in process design is complex gasification mechanism, since numerous phenomena at extreme process conditions take place simultaneously. This study is focused on integrated thermodynamic and artificial neural network approach (ANN) for entrained flow gasification kinetics investigation. Data on 102 feedstock materials composition was used in AspenPlus gasification simulation, where sensitivity analysis was performed for different equivalence ratio (0.1-0.7) and gasification temperature (1200-1500°C) values. For analyzed materials, optimal equivalence ratio range exist (usually 0.3-0.4), maximizing gasification efficiency. Obtained results were used in ANN development for each output variable (syngas composition, efficiency, heating value and carbon conversion). Matlab algorithm was used for determination of optimal number of neurons (1-20 range) in each ANN. High R^2 values (>0.99) for all models suggested good agreement between simulated and predicted values. Genetic algorithm-based optimization studies for maximization of hydrogen content and cold gas efficiency result in mean ER value of 0.35 and 0.41, respectively, at temperature of 1200°C. Yoon interpretation method was used for quantifying relative impacts of each input variable on syngas content and gasification efficiency. Proposed approach represents a powerful tool which can facilitate investigation of entrained flow gasification and process design.

Keywords: syngas, optimization, simulation, machine learning.

Highlights

- Sensitivity analysis of gasification kinetics of different feedstocks was performed in Aspen Plus
- Process parameters and feedstock impact on efficiency and syngas composition is analyzed
- Obtained results are used for ANN development and modeling with high accuracy
- Process parameters optimization studies regarding syngas content are performed

Introduction

Global energy production, despite an increase in renewable energy sources consumption, is still dominated by fossil fuels. Approximately one-third of global electricity production in 2022 came from renewable energy sources, while their share in total energy consumption is even lower, approaching 20% [1,2]. Taking into account non-renewable nature of fossil fuels and intensive greenhouse gas and pollutant emissions, energy industry is expected to shift towards cleaner energy sources (solar, wind, hydro, geothermal, biomass, etc.) [3], which is recognized and controlled by global policies [4,5]. Thus, serious effort is made in order to develop new and improve existing energy conversion technologies.

Thermochemical conversion technologies consist of the conversion of carbonaceous feedstocks into liquid, solid or gaseous products for further production of electricity, heat, chemicals or fuels. Among the conventional thermochemical conversion technologies (combustion, gasification and pyrolysis) [6], gasification offers benefits in terms of high conversion efficiency [7], achievable carbon capture and cleanup of produced gas (syngas) [8], as well as polygenerative potential due to specific syngas composition [9]. The process consists of partial oxidation of carbon in the fuel in the presence of a gasifying agent, such as oxygen, air, air-oxygen mixture, steam, steam-oxygen mixture or carbon-dioxide. Produced syngas consists mainly of carbon-monoxide, hydrogen, methane, carbon dioxide and water. Solid residue consists of ash and unconverted organic fraction of the fuel [10,11]. Overall reacting system is endothermic, where necessary energy can be provided by partial oxidation (auto-thermal gasification) or by external supply of energy (allo-thermal gasification). Considering the auto-thermal system, gasification can be seen as a sequence of three stages: drying, decomposition (devolatilization) and gasification. Overall process output depends on several factors, including operating conditions (temperature and pressure), amount and type of gasifying agent, feedstock composition and gasification technology [11,12].

Several gasification technologies have been developed in recent years, which differ in operating conditions, feedstock material state, capacity, efficiency and scale-up potential. Within the currently available gasification technologies, such as fixed bed and fluidized bed, entrained flow gasifiers constitute an interesting option owing to their commercial large-scale availability (technological readiness index of around 7-8), lower emissions and their high efficiency for the production of syngas [13,14]. Complex construction and operation, problems with construction materials at high temperatures, as well as fuel specificity in terms

of particle size, are compensated by high conversion efficiency, high capacity, good gas-solid contact and mixing, moderate heating value syngas and great scale-up potential. Typical entrained flow gasification (EFG) temperature is above ash melting point, typically in the range of 1200-1500°C, while gasification pressure is usually above 25 bar [13,15,16].

In order to develop and design gasification processes, detailed investigation of process kinetics must be done, which helps determine impact of operating conditions and feedstock material composition on outlet parameters, i.e., carbon conversion, syngas yield and syngas composition. Thus, several different gasification models have been developed, which can be divided into kinetic rate models, thermodynamic equilibrium models and neural network models [15]. Kinetic models provide essential information on kinetic mechanisms to describe the conversion during biomass gasification. Several studies that include kinetic models have been made, taking into account gasification reactions, heat and mass transfer and fluid dynamics in EFG [17–24]. Thermodynamic equilibrium models are independent of gasifier design and may be more suitable for process studies on the influence of the most important process parameters. Additionally, this model requires less details of the system in hand. Thus, stoichiometric and non-stoichiometric equilibrium models have extensively been used for gasification purposes [25–29], especially in the domain of EFG, since the system approaches thermodynamic equilibrium at higher temperatures [15,30]. Furthermore, this approach is often implemented in AspenPlus simulation software, which has become a standard procedure for simulation and investigation of gasification process. Software enables equilibrium calculations through Gibbs free energy minimization [30]. Artificial neural networks (ANN) have recently been successfully used in various areas of chemical engineering research. The concept of ANN allows for black-box modeling of large amount of data, which can be useful in phenomenologically complex processes, such as EFG and gasification in general. Therefore, several types of researches using ANN have been conducted in order to evaluate performance of various gasification systems [31], optimize a given gasification process for hydrogen production [32], model biomass gasification in fluidized bed gasifiers [33] and fixed bed downdraft gasifiers [34], predict biomass gasification process parameters [35], and develop a comprehensive gasification model, taking into account wide range of inlet and outlet parameters [36]. Also, some studies have developed an integrated thermodynamic equilibrium and ANN approach, which uses equilibrium calculations results as ANN input data, while single output variable is considered, mainly syngas heating value [37] and net energy output [38].

By using a simulation software like AspenPlus, thermodynamic equilibrium approach can be applied for gasification of different feedstock materials at different operating conditions. Thus, obtained data on syngas composition can be used for development of ANN, which will take into account feedstock composition, gasifying agent type and flowrate, as well as operating conditions and provide outputs in form of syngas composition, gasification efficiency, etc. This approach can be beneficial on multiple levels, since only obtained ANN models are necessary for evaluation of gasification performance, thus providing a tool for engineers for preliminary assessment of potential plant efficiency, gasification operation feasibility and necessary operating conditions. Also, gasification kinetics for a given material can be assessed without the use of process simulator, while comparative analysis of behavior of different feedstock materials can be performed.

It is worth mentioning that there is ongoing research and development in the field of gasification, and new and innovative technologies are emerging that could potentially surpass EFG in terms of efficiency and cost-effectiveness [39–41]. Nonetheless, EFG remains one of the most promising and widely used gasification technologies at present. Therefore, the goal of this research is to investigate in detail the kinetics of EFG process via integrated ANN and thermodynamic equilibrium approach. In order to obtain representative data on EFG, numerous different feedstock materials have been investigated, which composition is taken from the literature and used as an input in AspenPlus gasification simulation. Typical oxyfuel gasification process flowsheet configuration was used, while sensitivity analysis was performed for all samples, with equivalence ratio and gasification temperature as parameters to be varied. Obtained results are used as input data for ANN development using a Matlab algorithm for network topology optimization. Obtained models for prediction of output variables (syngas composition, cold gas efficiency, carbon conversion and syngas LHV) are further used for developing the objective function for optimization via genetic algorithm method. Objective function uses equivalence ratio and temperature as decision variables and parameter of interest as target variable, thus allowing for quick determination of optimal process parameters for a given feedstock material.

Materials and methods

Feedstock material data

In order to develop a comprehensive gasification model, wide range of input parameters is necessary. Since gasification is suitable for relatively broad spectrum of raw materials, data

on various feedstock material types composition is obtained from the literature. The general idea is to obtain data on proximate and ultimate analysis for materials of different origin and heating value, providing necessary range of individual components composition. Data on proximate and ultimate analysis is obtained for 40 municipal solid waste (MSW) and refuse derived fuel (RDF) samples, 39 biomass samples, 10 coal samples, and 13 biomass briquettes samples. Complete input data is given in Supplementary material, Table S1. Since further calculations require the data on materials lower heating value (*LHV*), for instances where only higher heating value (*HHV*) is given, necessary conversion is made according to Eq. 1 [42]:

$$LHV = HHV - (9 \cdot H + Moisture) \cdot 2.44 \quad \left[\frac{MJ}{kg}\right] \tag{1}$$

where *H* and *Moisture* stand for hydrogen and moisture content, respectively.

Process simulation and sensitivity analysis

Gasification process simulation is performed in AspenPlus software. Raw material composition data is used in definition of nonconventional components, with HCOALGEN and DCOALIGT models being used for enthalpy and density calculations. Peng-Robinson equation of state was used as a thermodynamic model. Defined components consist of nonconventional components (raw material and ash), decomposition products (C, H_2, N_2, H_2O, S, Cl_2, O_2) and possible syngas components (CH_4, CO, CO_2, NO, NH_3, HCl, H_2S, C_2H_6). Typical gasification process flowsheet (see Figure 1) is developed, where feedstock material (FEEDSTOCK) first enters the decomposition (DECOMP - Ryield) reactor, where drying and devolatilization processes take place at 500 °C and gasification pressure of 25 bar. Then, the mixture enters the gasification reactor (GASIFIER - RGibbs), along with pure oxygen (O2-GASIF), which enters the reactor at 200°C and 25 bar. In the gasifier, restricted chemical equilibrium calculations take place at the selected gasification temperature, while the heat required for decomposition (Q) is provided from this reactor. Obtained products are sent to a separator block (SEPARATOR), where unconverted carbon and ash are removed (SLAG), thus simulating the formation of slag in the gasifier.

Figure 1.

For determination of necessary oxygen flow rate for each simulation, equivalence ratio (ER) was used, while all calculations were performed in a Calculator block. Equivalence ratio for oxyfuel gasification is defined as:

$$ER = \frac{(O/F)}{(O/F)_{st}} \tag{2}$$

Where O/F stands for actual ratio of oxygen to fuel, while $(O/F)_{st}$ stands for stoichiometric ratio. Sensitivity analysis was performed for every raw material, with ER and gasification temperature being the parameters to be varied. Temperature was varied in the range of 1200 °C to 1500 °C, with 15 °C increments, while ER was varied in the range of 0.1 to 0.7, with 0.03 increments. Defined flowsheet configuration is set for autothermal gasification regime; if the gasification reactor provides insufficient heat for decomposition (for example, when ER is too low, or when the material has a low heating value), error is reported, and these results were not taken into consideration. Simulation results include content of main syngas components (CO, H_2, CO_2, CH_4 and H_2O), while obtained data is used for calculation of syngas LHV, carbon conversion and cold gas efficiency (CGE). Carbon conversion and CGE are calculated from following equations:

$$CONV = \frac{m_{c,in} - m_{c,out}}{m_{c,in}} \cdot 100(\%) \tag{3}$$

$$CGE = \frac{m_{syngas} \cdot LHV_{syngas}}{m_f \cdot LHV_f} \cdot 100(\%) \tag{4}$$

where $m_{c,in}$ and $m_{c,out}$ stand for carbon flow rate at gasifier inlet and outlet, m_{syngas} and m_f stand for syngas and feedstock mass flowrate, and LHV_{syngas} and LHV_f stand for syngas and feedstock LHV, respectively.

Artificial neural network modeling and optimization

Sensitivity analysis results are used as input data for development of ANN for prediction of output parameters. MatLab's Neural Network Toolbox was used for design of neural network structure. Standard structure with one hidden layer was used, with linear transfer function at the output layer and tangent sigmoid function at hidden layer. An algorithm was developed for determination of most suitable number of neurons in a hidden layer. The number of hidden neurons was varied from 1 to 20, and the training process of each network was run 10

times with random initial values of weights and biases. Best topology was determined according to coefficient of determination (R^2), Mean squared error (*MSE*) and mean absolute percentage error (*MAPE*) values. Bayesian regularization backpropagation algorithm was used for network training, where 60% of data was used as training data, 20% as validation data and 20% as test data. Each network consists of multiple inputs (ultimate analysis of feedstock material, moisture content, ER and temperature) and singular output (syngas content of a selected component (CH_4, CO_2, CO, H_2, H_2O), syngas LHV, CGE or carbon conversion). Hence, 8 independent ANNs were developed.

Obtained functions are later used for process optimization for a given condition using a genetic algorithm function. As a result of optimization procedure for a given feedstock material composition, the algorithm returns values for ER and gasification temperature. Therefore, the algorithm can be used for various problems, for example, in maximization or minimization of specific component content in syngas, in adjusting of components ratio in syngas, in maximization of CGE, syngas heating value or carbon conversion.

Results and discussion

Characteristics of investigated feedstock materials

As stated previously, materials of different origin were used in this study, in order to cover a wide range of elemental components compositions. It should be mentioned that some of the materials were completely unsuitable for gasification process, since the simulation reported errors for every combination of ER and temperature in sensitivity analysis. This is mainly due to high moisture content and low LHV value, which is typical for some MSW and biomass samples. General characteristics of feedstock material which were suitable for gasification simulation are shown in Figure 2. It should be noted that box plot for chlorine content was not displayed due to its low content in all materials. Also, outliers in LHV, carbon and sulfur content data correspond to coal samples used in this study.

Figure 2.

Impact of operating conditions on entrained flow gasification

In order to analyze and discuss relative impact of main operating conditions, ER and temperature on oxyfuel EFG process, results of a sensitivity study on a randomly selected feedstock material will be displayed. Surface plots for selected output parameters, mainly

syngas composition and overall gasification parameters, are displayed in Figures 3 and 4. According to plots displayed in Figure 3, nonlinear correlation between syngas composition and operating conditions can be observed. Crucial observation is that there is a distinctive range of operating parameters values for which H_2 and CO content are at maximum.

Figure 3.

Hydrogen content reaches maximum values in ER range of 0.33-0.4 (Figure 3a), while lower temperatures favor hydrogen content increase. Maximum CO content is obtained in similar ER range (Figure 3c), while further increase of ER value slightly decreases CO content, with similar conclusions about temperature influence to be made. It can be assumed that the dominant reactions in selected operating conditions range are partial oxidation and water-gas reactions. Methane content is significant at lower ER values (Figure 3b), where methanation and hydrogasification reactions are dominant. Methane and CO_2 content decrease with increase of ER (Figures 3b and 3d), with sharp decrease being in line with area of maximum H_2 / CO values.

Figure 4.

Overall gasification efficiency is strongly dependent on content of main syngas components, H_2 and CO, due to their high heating values. Cold gas efficiency increases with increase in ER, with maximum CGE values being in the ER range of 0.33-0.4 and lower temperature area (Figure 4b). Complete carbon conversion is obtained after the 0.35 ER threshold, for all temperatures (Figure 4c). In general, higher gasification temperatures lower the conversion and CGE, due to increase of necessary mixture sensible heat. It could be noted that the optimal operating conditions ensure complete carbon conversion with minimal consumption of gasifying agent. Syngas LHV follows the similar pattern, with main difference being in a significant decrease in high ER area (Figure 4a). However, higher ER results in higher overall gas yield, which explains slight decrease in CGE values (see Eq. 4 and Figure 4b).

Gasification kinetics in general is complex, since the process takes place via series of elementary reactions. However, it is stated in the literature that few global reactions, including only key components and interproducts can be used for modeling purposes. Those reactions are given in Table 1 [43].

Table 1.

Simulation results indicate that high hydrogen content corresponds to low water content in syngas, which can be attributed to water-gas shift reaction, as well as steam gasification reaction, where carbon is gasified with water vapor. At the area of complete carbon conversion, carbon gasification and oxidation no longer take place, which also causes hydrogen not to form via steam gasification reaction. Boudouard reaction is one of the most important reactions in entire gasification mechanism, where carbon reacts with CO_2 while forming CO. This explains decrease of CO content in the area of higher ER. At complete carbon conversion, system stabilizes and no significant composition changes take place. Only homogenous reactions take place, primarily water-gas shift, while temperature and approximately equilibrium composition prohibit further reaction advancement. Also, it is important to highlight that methane and other hydrocarbons decompose at higher temperatures [13], which is why the obtained methane content is low.

3.3 Artificial neural networks

One neural network was developed for each output variable via algorithm described in Section 2.3. It should be noted that after initial runs, the number of input parameters were decreased, since chlorine and nitrogen content in feedstock materials is very low and their impact on output variables should be negligible (due to small quantity and inert nature of their gasification products). Likewise, ash is inert in gasification process, thus, its impact is also neglected, resulting in 7 input parameters (carbon, hydrogen, oxygen, sulfur and moisture content, ER and gasification temperature) for each output parameter. ANNs performance and topology are shown in Table 2, while parity plots of some predicted and simulated values are shown in Figure 5. Remaining parity plots are given in Supplementary material, Figure S1.

Table 2.

Number of hidden neurons increases the prediction accuracy, since optimal number of neurons was close to 20, while coefficients of determination values were above 0.99 for all instances. The impact of hidden neurons' number on coefficient of determination for each neural network is given in Supplementary material, Figures S2 and S3. High accuracy is also confirmed by low MSE and MAPE values. It should be noted that simulated values of certain values are close to zero for a wide range of operating parameters, thus resulting in a relatively high MAPE value, even though overall prediction accuracy is high.

Figure 5.

To quantify the impact of input variables on syngas composition and overall gasification parameters, Yoon's interpretation method was used [44]. Obtained results are displayed in Table 3. In can be noted that equivalence ratio has a higher general impact on syngas composition and overall gasification efficiency than temperature, while carbon and moisture content impact the syngas composition the most. Results on relative importance of ER and gasification temperature are in line with sensitivity analysis results displayed previously.

Table 3.

Since developed neural network models show good agreement between simulated and predicted data, they could be further used for optimization purposes. Two optimization problems were tested; obtaining the maximum hydrogen fraction in syngas and obtaining of maximum CGE for a given feedstock material. Genetic algorithm was used for optimization on each feedstock material, with ER and gasification temperature as output parameters. Parity plots on simulated (based on sensitivity analysis results) and predicted (optimization) hydrogen fraction and CGE are shown in Figure 6.

Figure 6.

Obtained optimization results are in accordance with sensitivity analysis results. It should be noted that ER and temperature are in this case continuous variables, contrary to sensitivity analysis, which could lead to slight deviation of results. Temperatures corresponding to optimal operating conditions are close to minimal gasification temperature of 1200°C, while mean ER values are 0.35 for hydrogen optimization and 0.41 for CGE optimization.

In general, this approach contributes to better understanding of EFG process kinetics, while developed ANN models can be used for quick prediction of gasification output parameters for a given feedstock. Obtained syngas composition can be futher used to facilitate gasification based processes simulation, since complex three-phase calculations are bypassed. Also, models can be used for process optimization i.e. obtaining the optimal operating conditions for a specified goal.

Conclusion

An integrated ANN and AspenPlus gasification model was used for investigation of entrained flow gasification kinetics. Various feedstock materials, mainly waste, RDF, coal and biomass

were used in order to obtain a wide range of input material elemental compositions. For each feedstock material, sensitivity analysis on EFG in AspenPlus was performed, for different equivalence ratios and temperatures, and obtained results were used in ANN development. Single layer ANNs with adjustable number of neurons were developed for every output variable (syngas components fractions, cold gas efficiency, syngas lower heating value and carbon conversion), with high prediction accuracy (R^2>0.99). All models consists of high number of hidden neurons (19-20). Also, general impact of ER and temperature, as well as feedstock material composition on output parameters was determined and discussed. Highest gasification efficiencies are obtained at lower temperatures, just above ash melting temperatures, and in a narrow range of ER, typically 0.35-0.45, depending on feedstock material composition. In this ER range, highest H_2 content and moderate CO content is obtained, resulting in highest syngas heating value. Further increase of ER does not have a significant effect on syngas composition. Obtained models can be used for optimization problems, where two desired goals were succesfully tested; determination of optimal combination of ER and temperature for maximization of syngas hydrogen content and cold gas efficiency. For investigated materials, mean optimal parameters are temperature of 1200°C and ER of 0.41 and 0.35 for cold gas efficiency and hydrogen content, respectively. This combined ANN and simulation approach allows for quick and accurate prediction of EFG efficiency and syngas composition, thus providing essential information for design and development of gasification processes.

Acknowledgements: The authors would like to thank the Ministry of Education, Science and Technological Development of the Republic of Serbia, Project No. 451-03-65/2024-03/200134.

References

[1] H. Ritchie, P. Rosado, M. Roser, Energy Production and Consumption, https://ourworldindata.org/energy-production-consumption [accessed 7 May 2024].

[2] IEA, World Energy Outlook 2022, https://www.iea.org/reports/world-energy-outlook-2022 [accessed 7 May 2024].

[3] M.N. Dudin, E.E. Frolova, O.V. Protopopova, O. Mamedov, S.V. Odintsov, 6 (2019) 1704. https://doi.org/10.9770/jesi.2019.6.4(11).

[4] C.-F. Schleussner, J. Rogelj, M. Schaeffer, T. Lissner, R. Licker, E.M. Fischer, R. Knutti, A. Levermann, K. Frieler, W. Hare, Nat Clim Chang 6 (2016) 827–835. https://doi.org/10.1038/nclimate3096.

[5] L. Mundaca, L. Neij, A. Markandya, P. Hennicke, J. Yan, Appl Energy 179 (2016) 1283–1292. https://doi.org/10.1016/j.apenergy.2016.08.086.

[6] H.B. Goyal, D. Seal, R.C. Saxena, 12 (2008) 504–517. https://doi.org/10.1016/j.rser.2006.07.014.

[7] V. Kirubakaran, V. Sivaramakrishnan, R. Nalini, T. Sekar, M. Premalatha, P. Subramanian, 13 (2009) 179–186. https://doi.org/10.1016/j.rser.2007.07.001.

[8] V. Tola, A. Pettinau, Appl Energy 113 (2014) 1461–1474. https://doi.org/10.1016/j.apenergy.2013.09.007.

[9] J. Parraga, K.R. Khalilpour, A. Vassallo, 92 (2018) 219–234. https://doi.org/10.1016/j.rser.2018.04.055.

[10] R. Rauch, J. Hrbek, H. Hofbauer, Wiley Interdiscip Rev Energy Environ 3 (2014) 343–362. https://doi.org/10.1002/9781118957844.ch7.

[11] A. Molino, S. Chianese, D. Musmarra, 25 (2016) 10–25. https://doi.org/10.1016/j.jechem.2015.11.005.

[12] M. Lapuerta, J.J. Hernández, A. Pazo, J. López, 89 (2008) 828–837. https://doi.org/10.1016/j.fuproc.2008.02.001.

[13] U. Arena, 32 (2012) 625–639. https://doi.org/10.1016/j.wasman.2011.09.025.

[14] J.J. Hernández, G. Aranda-Almansa, A. Bula, 91 (2010) 681–692. https://doi.org/10.1016/j.fuproc.2010.01.018.

[15] M. Puig-Arnavat, J.C. Bruno, A. Coronas, 14 (2010) 2841–2851. https://doi.org/10.1016/j.rser.2010.07.030.

[16] E. Henrich, F. Weirich, Environ Eng Sci 21 (2004) 53–64. https://doi.org/10.1089/109287504322746758.

[17] T. Xu, Y. Wu, S. Bhattacharya, Int J Min Sci Technol 31 (2021) 473–481. https://doi.org/10.1016/j.ijmst.2021.03.001.

[18] F. Qian, X. Kong, H. Cheng, W. Du, W. Zhong, Ind Eng Chem Res 52 (2013) 1819–1828. https://doi.org/10.1021/ie301630x.

[19] M. Vascellari, R. Arora, C. Hasse, 118 (2014) 369–384. https://doi.org/10.1016/j.fuel.2013.11.004.

[20] G.-S. Liu, H.R. Rezaei, J.A. Lucas, D.J. Harris, T.F. Wall, 79 (2000) 1767–1779. https://doi.org/10.1016/S0016-2361(00)00037-5.

[21] A. Tremel, H. Spliethoff, 107 (2013) 170–182. https://doi.org/10.1016/j.fuel.2013.01.062.

[22] M. Vascellari, D.G. Roberts, D.J. Harris, C. Hasse, 152 (2015) 58–73. https://doi.org/10.1016/j.fuel.2015.01.038.

[23] I. Adeyemi, I. Janajreh, Renew Energy 82 (2015) 77–84. https://doi.org/10.1016/j.renene.2014.10.073.

[24] M.A. Kibria, P. Sripada, S. Bhattacharya, 196 (2020) 117073. https://doi.org/10.1016/j.energy.2020.117073.

[25] M. Al-Zareer, I. Dincer, M.A. Rosen, 115 (2016) 1–18. https://doi.org/10.1016/j.cherd.2016.09.009.

[26] M. Pérez-Fortes, A.D. Bojarski, E. Velo, J.M. Nougués, L. Puigjaner, 34 (2009) 1721–1732. https://doi.org/10.1016/j.energy.2009.05.012.

[27] Y. Lu, Z. Li, M. Zhang, C. Huang, Z. Chen, Energy Convers Manag 245 (2021) 114627. https://doi.org/10.1016/j.enconman.2021.114627.

[28] Z. Dai, X. Gong, X. Guo, H. Liu, F. Wang, Z. Yu, 87 (2008) 2304–2313. https://doi.org/10.1016/j.fuel.2007.12.005.

[29] D. Barba, M. Prisciandaro, A. Salladini, G.M. Di Celso, 90 (2011) 1402–1407. https://doi.org/10.1016/j.fuel.2010.12.022.

[30] Ö.Ç. Mutlu, T. Zeng, Chem Eng Technol 43 (2020) 1674–1689. https://doi.org/10.1002/ceat.202000068.

[31] M. Ozonoh, B.O. Oboirien, A. Higginson, M.O. Daramola, Renew Energy 145 (2020) 2253–2270. https://doi.org/10.1016/j.renene.2019.07.136.

[32] H.O. Kargbo, J. Zhang, A.N. Phan, Appl Energy 302 (2021) 117567. https://doi.org/10.1016/j.apenergy.2021.117567.

[33] M. Puig-Arnavat, J.A. Hernández, J.C. Bruno, A. Coronas, Biomass Bioenergy 49 (2013) 279–289. https://doi.org/10.1016/j.biombioe.2012.12.012.

[34] D. Baruah, D.C. Baruah, M.K. Hazarika, Biomass Bioenergy 98 (2017) 264–271. https://doi.org/10.1016/j.biombioe.2017.01.029.

[35] R. Mikulandrić, D. Lončar, D. Böhning, R. Böhme, M. Beckmann, Energy Convers Manag 87 (2014) 1210–1223. https://doi.org/10.1016/j.enconman.2014.03.036.

[36] S. Ascher, W. Sloan, I. Watson, S. You, Appl Energy 320 (2022) 119289. https://doi.org/10.1016/j.apenergy.2022.119289.

[37] F. Kartal, U. Özveren, 209 (2020) 118457. https://doi.org/10.1016/j.energy.2020.118457.

[38] S. Safarian, S.M.E. Saryazdi, R. Unnthorsson, C. Richter, 213 (2020) 118800. https://doi.org/10.1016/j.energy.2020.118800.

[39] J. Chen, J. Liang, Z. Xu, E. Jiaqiang, Energy Convers Manag 226 (2020) 113497. https://doi.org/10.1016/j.enconman.2020.113497.

[40] H. Shahbeik, W. Peng, H.K.S. Panahi, M. Dehhaghi, G.J. Guillemin, A. Fallahi, H. Amiri, M. Rehan, D. Raikwar, H. Latine, 167 (2022) 112833. https://doi.org/10.1016/j.rser.2022.112833.

[41] M. Shahbaz, T. Al-Ansari, M. Inayat, S.A. Sulaiman, P. Parthasarathy, G. McKay, 134 (2020) 110382. https://doi.org/10.1016/j.rser.2020.110382.

[42] A. Ozyuguran, A. Akturk, S. Yaman, 214 (2018) 640–646. https://doi.org/10.1016/j.fuel.2017.10.082.

[43] A. Gómez-Barea, P. Ollero, B. Leckner, 103 (2013) 42–52. https://doi.org/10.1016/j.fuel.2011.04.042.

[44] Y. Yoon, G. Swales Jr, T.M. Margavio, 44 (1993) 51–60. https://doi.org/10.1057/jors.1993.6.

Figure captions

Figure 1 AspenPlus gasification process flowsheet

Figure 2. Box-plot representation of feedstock materials composition and LHV taken from literature; *db* stands for dry-basis composition

Figure 3. Dry-basis a) H_2 content, b) CH_4 content, c) CO content, d) CO_2 content in syngas as a function of ER and gasification temperature

Figure 4. Overall gasification parameters, a) syngas LHV, b) CGE, c) carbon conversion as a function of ER and gasification temperature

Figure 5. Simulated and predicted data on a) H_2 content, b) CO content, c) syngas LHV and d) CGE, according to developed artificial neural network model

Figure 6. Predicted and simulated a) H_2 content and b) CGE according to optimization procedure

Table 1. Main gasification reactions

Stoichiometry	**Name**
Char combustion	
$C+1/2O_2 \rightarrow CO$	Partial combustion
$C+O_2 \rightarrow CO_2$	Complete combustion
Char gasification	
$C+CO_2 \rightarrow 2CO$	Boudouard reaction
$C+H_2O \rightarrow CO+H_2$	Steam gasification
$C+2H_2 \rightarrow CH_4$	H_2 gasification
Homogenous	
$CO+1/2O_2 \rightarrow CO_2$	CO oxidation
$H_2+1/2O_2 \rightarrow H_2O$	H_2 oxidation
$CH_4+2O_2 \rightarrow CO_2+2H_2O$	CH_4 oxidation
$CO+H_2O \rightarrow CO_2+H_2$	Water-gas shift

Table 2. Artificial neural network structure and prediction accuracy

Each output neuron	Hidden neurons	R^2	MAPE %	MSE
H_2	19	0.9938	4.3858	$4.7553 \cdot 10^{-5}$
CO	19	0.9988	13.6318	$4.4521 \cdot 10^{-5}$
CH_4	19	0.9987	60.3509	$2.74339 \cdot 10^{-6}$
CO_2	20	0.9968	16.8125	$2.9776 \cdot 10^{-5}$
H_2O	20	0.9984	7.0330	$6.6187 \cdot 10^{-5}$
Syngas LHV	20	0.9997	0.4967	0.0035
CGE	20	0.9989	1.3559	0.6355
Carbon conversion	20	0.9994	0.2970	0.1951

Table 3. Relative impact of input parameters on output parameters in EFG process

	ER	**T, °C**	**C**	**H**	**O**	**Moisture**
H_2	38.0±12.5	-4.3±0.5	13.6±2.8	1.6±6.4	6.3±9.1	-17.4±4.5
CO	38.7±7.2	-3.8±0.6	11.5±4.2	3.0±7.8	4.0±3.8	-15.3±8.5
CH_4	-49.9±6.2	4.3±0.5	-12.4±1.6	5.7±2.7	-1.6±2.5	10.1±5.6
CO_2	-21.2±6.7	3.8±1.0	-7.5±7.8	-9.7±5.0	2.1±7.2	12.0±8.6
H_2O	-36.1±8.4	4.1±0.6	-16.3±4.3	-2.8±4.9	-2.0±4.4	23.3±3.1
Syngas LHV, MJ/kg	7.7±11.3	-3.6±0.9	4.5±4.4	20.0±5.0	-2.7±4.9	-14.3±6.6
CGE, %	4.2±5.3	-0.6±0.8	9.4±5.5	-9.7±17.3	-3.9±11.8	-7.1±6.6
Carbon conversion, %	39.7±7.4	-1.7±0.6	-1.3±2.9	7.5±4.1	9.5±3.7	9.3±5.3

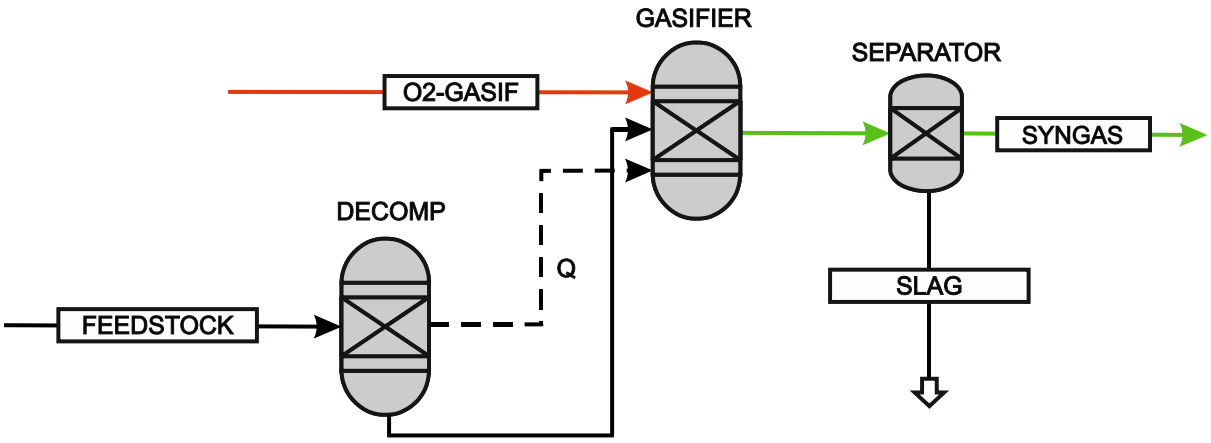
GASIFIER
SEPARATOR
O2-GASIF
SYNGAS
DECOMP
Q
SLAG
FEEDSTOCK

Figure 1.

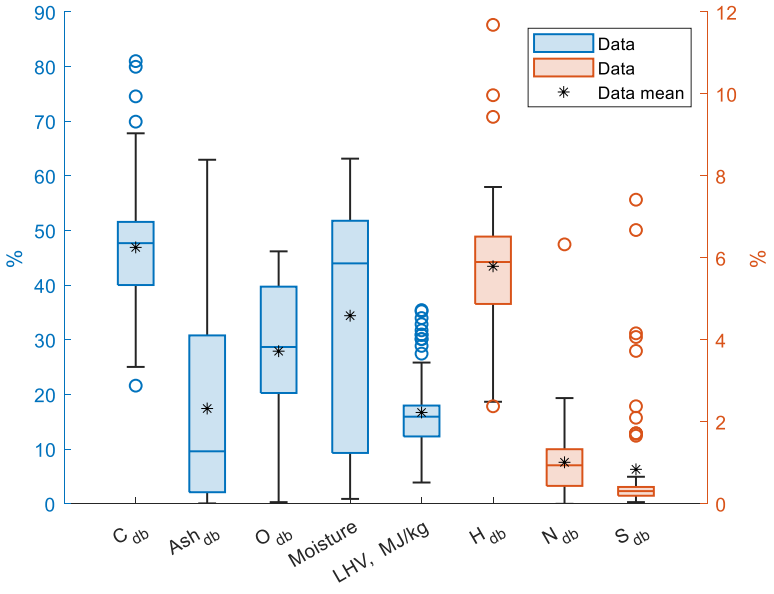
Data
Data
Data mean
%
%
C db
Ash db
O db
Moisture
LHV, MJ/kg
H db
N db
S db

Figure 2.

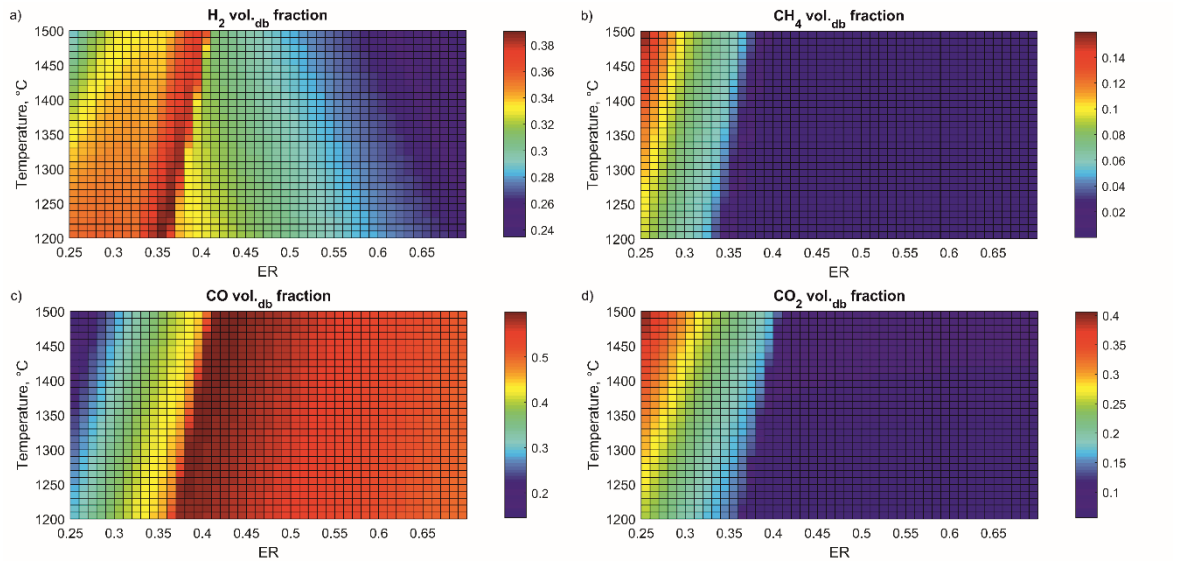
a)
H2 vol.db fraction
b)
CH4 vol.db fraction
c)
CO vol.db fraction
d)
CO2 vol.db fraction
Temperature, °C
ER

Figure 3.

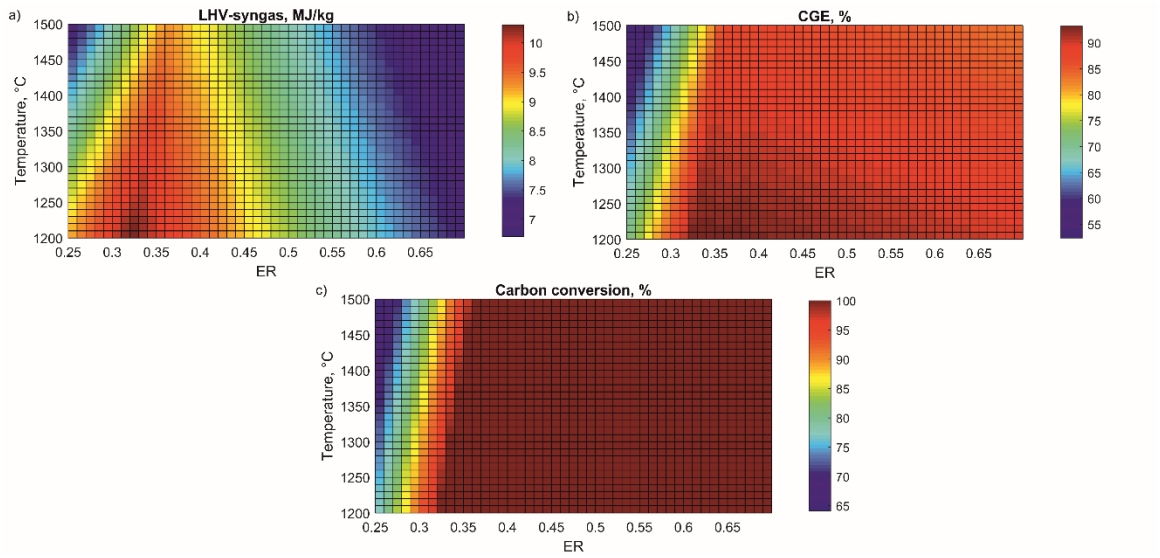
a)
LHV-syngas, MJ/kg
Temperature, °C
ER
b)
CGE, %
Temperature, °C
ER
c)
Carbon conversion, %
Temperature, °C
ER

Figure 4.

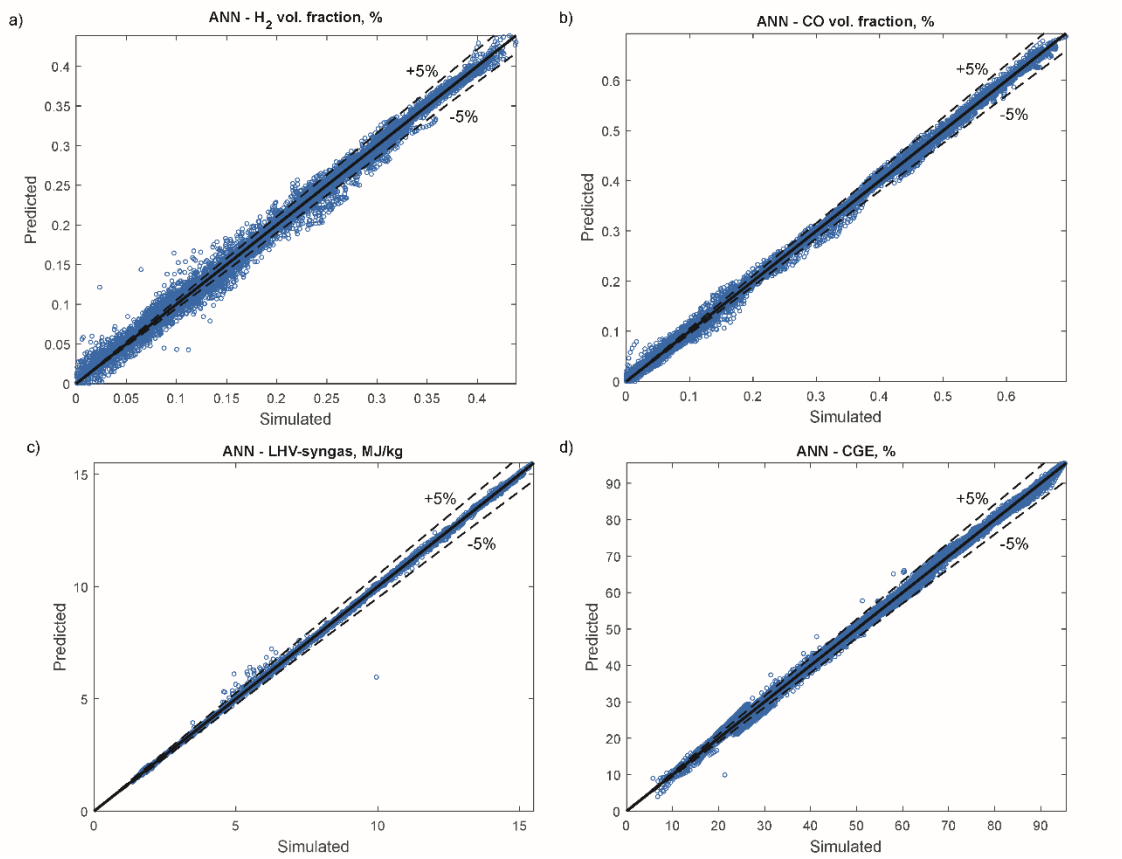
a)
ANN - H2 vol. fraction, %
+5%
-5%
Predicted
Simulated
b)
ANN - CO vol. fraction, %
+5%
-5%
Predicted
Simulated
c)
ANN - LHV-syngas, MJ/kg
+5%
-5%
Predicted
Simulated
d)
ANN - CGE, %
+5%
-5%
Predicted
Simulated

Figure 5.

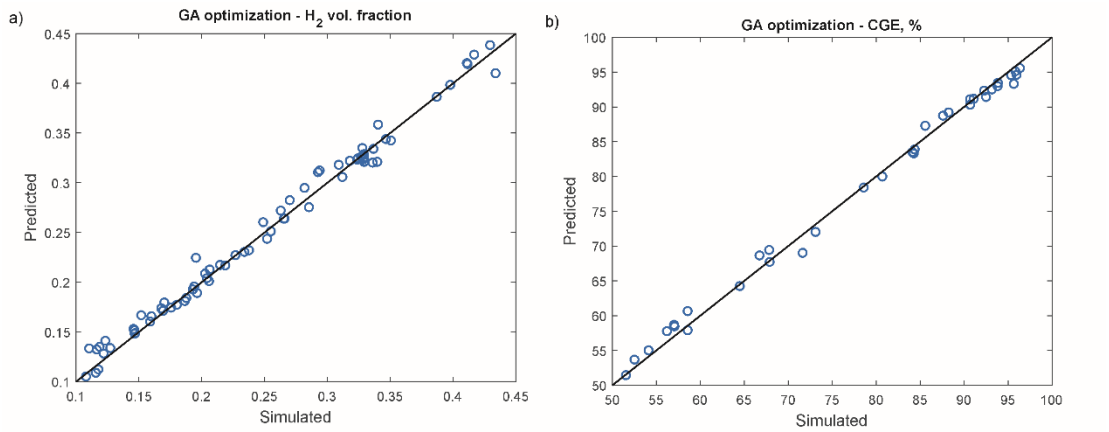
a)
GA optimization - H2 vol. fraction
Predicted
Simulated
0.1
0.15
0.2
0.25
0.3
0.35
0.4
0.45
b)
GA optimization - CGE, %
Predicted
Simulated
50
55
60
65
70
75
80
85
90
95
100

Figure 6.